25th Australasian Conference on Mechanics of Structures and Materials (ACMSM25)
Edited by C.M. Wang, J.C.M. Ho and S. Kitipornchai
Brisbane, Australia, December 4 – 7, 2018

NUMERICAL INVESTIGATION ON HOLLOW PULTRUDED FIBRE REINFORCED POLYMER TUBE COLUMNS

A. AL-SAADI *, T. ARAVINTHAN and W. LOKUGE

Centre for Future Materials (CFM), School of Civil Engineering and Surveying, University of Southern Queensland, QLD 4350, Australia
Emails: AliUmranKadhum.Alsaadi@usq.edu.au, Thiru.Aravinthan@usq.edu.au, Weena.Lokuge@usq.edu.au
* Corresponding author

Abstract. *As the axial behaviour of hollow pultruded fibre reinforced polymer (PFRP) profiles is governed by the instability conditions due to the local and global buckling, the determination of the safe load carrying capacity of FRP columns is vital. The compressive performance of PFRP tube depends on many factors such as fibre type, fibre content, and orientation of fibre layers, cross-section, thickness and height of the column member.*

In this study, concentric compressive testing was conducted using PFRP short columns. Based on the fibre orientation and thickness, the samples were divided into two groups of tubes in a square shape and two groups in a circular shape. The height of columns is designed to keep the slenderness ratio (length/lateral dimension) of 5. The axial behaviour of FRP columns was simulated using STRAND7 finite element software package. The laminate method was followed to define the mechanical properties of the FRP material. Failure was investigated by using the Tsai-Wu failure criterion.

The experimental results show that the failure mode of the hollow square tube was either local buckling or corner splitting at the mid-height followed by buckling. Although both types of circular tubes failed in a similar way by crushing one end with high noise, followed by separation of the crushed end into strips, the stiffness and the load capacity of PFRP column was higher for the profiles with fibres oriented close to the axial direction. The numerical results are in close agreement with the peak value of the experimental results. This can be extended to study the effects of all factors that influence the axial behaviour of PFRP columns numerically.

Keywords: Axial behaviour; Buckling; Column; Finite element; Pultruded FRP tube.

1 INTRODUCTION

The attractive properties of the composite material such as high strength-weight ratio, corrosion resistance and no maintenance cost have triggered researchers for spreading the use of FRP composite materials in the construction industry. Pultruded FRP profiles that are made in shapes similar to those made of steel can be used as an axial compressive column member. The instability conditions due to local or global buckling prevent the FRP profiles to reach their potential strength capacities. One of the necessary requirements for considering the FRP profiles as a constructional axial compression member is to calculate the load carrying capacity by taking into account the effects of instability conditions.

The first approach followed by researchers is to conduct an experimental test on different shapes of pultruded FRP sections to study their axial behaviour and then propose an analytical model to determine the load capacity (Barbero & Tomblin 1994; Zureick & Scott 1997; Hassan & Mosallam 2004; Puente et al. 2006). The second approach assumed the local buckling as a plate buckling problem and conducted an analytical study of FRP plate element by considering different kinds of loading and various states of restraint (Kollár 2002, 2003; Ragheb 2017). However, the cost-effective alternative approach is using finite element analysis. The previous studies have dealt with FRP material as an orthotropic material (Youssf et al. 2014; Abdelkarim & Elgawady 2015) with or without considering the stiffness in the axial direction (Jiang & Wu 2012; Teng et al. 2015). The concept of the lamina level to define the properties of the FRP material in the finite element was adopted by few researchers (Carrion et al. 2005; Guades et al. 2014; Hany et al. 2016).

In this study, finite element simulation to observe the axial behaviour of circular and square pultruded FRP tubes is presented. The approach used to define the FRP properties in the finite element is lamina method. Although this method provides ability to reform the stacking sequence of the laminate layers, laminate thickness and laminate properties in axial and transverse directions, it needs specific data regarding the laminate units in building FRP lamina. The necessary data are the number of fibre layers, their thickness and orientation and mechanical properties of the lamina.

2 SIMULATION METHODOLOGY

Four types of pultruded square and circular FRP tubes were tested to study the effect of fibre orientation, wall thickness and cross-sectional shape (Fig.1). All tubes are made of glass fibre and vinyl-ester resin except square tube S2 which is fabricated by using polyester resin. Table 1 shows the geometry and dimensions of pultruded FRP tubes.

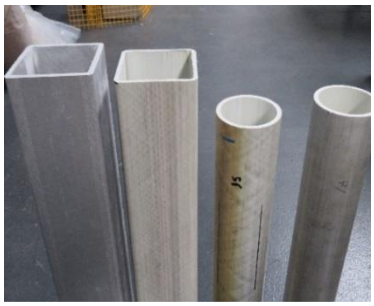

Figure 1 Pultruded FRP tubes.

Table 1 Dimensions and properties of pultruded tubes

	Unit	S1	S2	C1	C2
Shape		Square	Square	Circular	Circular
Dimensions	mm	100x100, t=5.2	102x102, t=6.4	d=88.9, t= 6.0	d=88.9, t= 6.0
Fibre content (from burnout test)	%	77.3	72.2	79.5	78.3
Fibre content (from manufacturer)	%	77.4	70.0	77.4*	77.4*
Density	g/cm^3	1.943	2.007	2.058	2.082
Fibre orientation	Degrees	0, +50, -50	0, +45, -45	0, +56, -56	0, +71, -71
Equivalent thickness	mm	4.30, 0.45, 0.45	5.20, 0.60, 0.60	4.50, 0.75, 0.75	3.44, 1.28, 1.28

*The fibre content was assumed as that of the square tube (S1).

The fundamental data to calculate the mechanical properties of FRP laminate can be assessed by conducting burnout tests based on ISO-1172 (1996) standard. The number of fibre layers, their orientation and thickness and mechanical properties of uni-directional FRP lamina are the required input parameters for finite element program. The stacking sequences of FRP laminate can be identified by separating layers one after the other. The weight of each layer is also measured. Finally, the calculated thickness value of each fibre orientation is computed by multiplying the total laminate thickness with the ratio of the individual layer weight to total weight of the fibre content (Table 1).

3 FINITE ELEMENT SIMULATION

The GFRP composite laminate consists of a number of unidirectional lamina which is stacked together in different orientations. The mechanical properties of the GFRP lamina that are used in the finite element analysis can be obtained either through performing experimental coupon tests of the lamina or by using micromechanical equations. The latter approach provides reasonable estimates of particular elastic properties (Carrion et al. 2005). The necessary properties of the lamina are elastic modulus in the fibre direction (E1), the elastic modulus in the transverse direction (E2), Poisson's ratio (υ12) and in-plane shear modulus (G12).By assuming a perfect bond between fibres and matrix, the axial strain of fibres and strain of the matrix are equal and uniform. Thus, the longitudinal properties (E1 and υ12) can be estimated by using the rule of mixtures as follows ((Carrion et al. 2005; Daniel 2006; Barbero 2017):

$$E_1 = E_f V_f + E_m (1\text{-}V_f) \quad (1)$$

$$\nu_{12} = \nu_f V_f + \nu_m (1\text{-}V_f) \quad (2)$$

Where E_f and E_m are the longitudinal fibre and matrix moduli, respectively. ν_f, ν_m are the Poisson's ratio of the fibres and matrix respectively, and V_f is the volume fractions of fibre.

For the other lamina properties (E_2, G_{12}), the rule of the mixture does not provide a good estimation as the stress in the matrix is non uniform . Thus, researchers have developed semi empirical approaches to obtain better approximations. The relationship of Halpin-Tsai for the transverse modulus and in plane shear modulus are considered in this study (Daniel 2006).

$$E_2 = E_m \frac{(1+V_f)E_{2f}+V_m E_m}{V_m E_{2f}+(1+V_f)E_m} \quad (3)$$

$$G_{12} = G_m \frac{(1+V_f)G_{12f}+V_m G_m}{V_m G_{12f}+(1+V_f)G_m} \quad (4)$$

E_m and E_{2f} are the matrix and transverse fibre moduli respectively, and V_m is the volume fraction of the matrix. G_m and G_{12f} are the shear modulus of the matrix and fibre respectively. In the same way, the intralaminar shear modulus (G_{23}) can be computed from equations (5) and (6) while the (G_{13}) is assumed to be equal to (G_{12}) (Barbero 2017).

$$G_{23} = G_m \frac{V_f + \eta(1-V_f)}{\eta(1-V_f)+(V_f G_m/G_{12f})} \quad (5)$$

$$\eta = \frac{3 - 4\nu_m + (G_m/G_{12f})}{4(1-\nu_m)} \quad (6)$$

To apply these equations, the mechanical properties and volume fractions of both fibre and matrix should be determinedtogether with the orientation of plies. The standard tabulated values of fibre and matrix which are given in the past (Daniel 2006; Barbero 2017) are adopted in this

study.The mechanical properties of fibre and matrix that are considered to calculate the unidirectional lamina properties can be shown in Table 2.

Table 2 Mechanical properties of glass fibre and matrix

E-glass fibre				Vinyl- Ester resin			Polyester resin		
E_{1f} (MPa)	E_{2f} (MPa)	G_{12f} (MPa)	ν_f	E_m (MPa)	G_m (MPa)	ν_m	E_m (MPa)	G_m (MPa)	ν_m
73000	73000	30000	0.23	3000-4000	1100-1500	0.35	3200-3500	700-2000	0.35

The fibre mass fraction and matrix mass fraction obtained from burnout test are used to calculate the fibre and matrix volume fractions. The fibre volume fraction was assumed to be uniform for all plies.

3.1 Material Properties

The mechanical properties of the uni-directional FRP lamina were calculated using the micromechanical equations presented above for all pultruded FRP tubes. The values of fibre content of providers are used in calculations. Table 3 shows values of modulus in fibre direction ($\boldsymbol{E_1}$), modulus in transverse direction ($\boldsymbol{E_2}$), Poisson's ratio ($\boldsymbol{\upsilon_{12}}$), in-plane shear modulus ($\boldsymbol{G_{12}}$) and out-plane shear modulus ($\boldsymbol{G_{23}}$). It should be noted that the average values of resin are used in calculations.

Table 3 Calculated mechanical properties of FRP lamina

FRP tube	($\boldsymbol{E_1}$) GPa	($\boldsymbol{E_2}$) GPa	($\boldsymbol{\upsilon_{12}}$)	($\boldsymbol{G_{12}}$) GPa	($\boldsymbol{G_{23}}$) GPa
S1,C1,C2	45.7	12.1	0.28	4.6	4.0
S2	41.3	9.9	0.28	4.0	3.6

3.2 Element Type and Failure Criteria

Four-node plate/shell elements were used to model the pultruded FRP tube in the finite element. The mesh was refined to ensure the continuity in the distribution of the stress and strains. The number of plate elements is 1250 and 1734 for thinner and thicker square tube respectively, and the number for circular tube was 540. The nonlinear static solver was followed. The stiffness of the plate elements according to its deformation was recalculated before each load step by considering the geometric nonlinearity.

The strength of FRP laminate relies on the strength of its building unit lamina. Thus, for design purposes, the value of load that initiates the ply failure is vital to limit the applied load below. Different failure criteria were proposed to predict the initiation of the first ply failure (FPF) (Barbero 2017). The Tsai-Wu failure theory has been used to predict the FPF of the pultruded GFRP tube. The expression of the Tsai-Wu theory is:

$$\frac{\sigma_t^2}{\sigma_{tt}\,\sigma_{tc}}+\frac{\sigma_a^2}{\sigma_{at}\,\sigma_{ac}}+\frac{\tau_{ta}^2}{\tau_{tap}^2}+\left(\frac{1}{\sigma_{tt}}-\frac{1}{\sigma_{tc}}\right)\sigma_t+\left(\frac{1}{\sigma_{at}}-\frac{1}{\sigma_{ac}}\right)\sigma_a-\frac{\sigma_a\sigma_t}{\sqrt{\sigma_{tt}\sigma_{tc}\sigma_{at}\sigma_{ac}}}=1 \qquad (8)$$

Where σ_t and σ_a are the transverse tensile stress and axial compressive stress of the FRP lamina respectively. τ_{ta} and τ_{tap} are the shear stress of FRP lamina and allowable shear stress respectively. σ_{tt} and σ_{tc} are the allowable transverse tensile and compressive strength of the FRP lamina respectively, σ_{at} and σ_{ac} are the allowable axial tensile and compressive strength of the FRP lamina respectively.

The failure will occur in any ply when the left side of equation (8) be equal to or greater than 1. In Strand7, the reserve factor was calculated to refer the state condition of each ply which is considered to be unsafe if the reserve factor is less than 1. This procedure was followed mainly for the circular hollow columns as they are not subjected to the local buckling. On the other hand, the hollow square columns experience local buckling before the stress in the FRP ply reaches limit value. The ultimate strength of the FRP lamina for pultruded GFRP tubes are listed in Table 4 noting that average values are considered in the finite element (Kollár & Springer 2003; *Module7: Strength and Failure Theories* 2014).

Table 4. Strength limits of FRP lamina

	Longitudinal strength (MPa)		Transverse strength (MPa)		Shear strength (MPa)
	Tension	Compression	Tension	Compression	
Glass- Vinyl ester	548	803	43.0	187	64.0
Glass-Polyester	650-950	600-900	20-25	90-120	45-60

3.3 Boundary Conditions and Loading

All degrees of freedom for nodes at upper and lower ends of the pultruded column were restrained except the axial deformation in the negative direction of Z-axis for upper end had been permitted. The boundary conditions of the symmetry planes (Z-Y) and (Z-X) were also added (Fig.2). The applied load was an axial displacement of the upper nodes in the negative Z-axis direction. The total displacement was applied in small steps to capture the reduction in the stiffness of the FRP tube due to the geometric deformation.

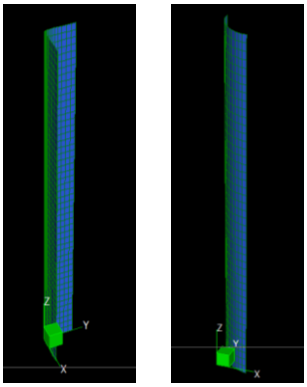

Figure 2 Finite element model

4. Results and discussion

A total of 4 column sets was simulated under axial concentric compressive load and compared with the experimental data available for the same type of columns. Fig.3 shows the axial load–axial displacement curves for column specimens. The experimental curves show that all columns behaved linearly before hitting the peak load but their response after peak load was reduced in a sharp manner. The finite element load-axial displacement curves are terminated when either the local buckling or first ply failure occurs. There is a reasonable estimation between numerical and experimental data in the pre-peak stage. The post–peak behaviour of columns cannot be captured by the simulation due to limitation of the program in updating the stiffness of FRP plate element after obtaining material failure. However, this limitation does not affect on results since the concentration is given to the value of the peak load.

The experimental peak-load values of the pultruded FRP square tube type S1 was 467.0 kN in an average of two specimens while the square tube S2 could reach up to 745.5 kN. The load carrying capacity of the circular tube C1 was 474.2 kN as an average of identical specimens. On the other hand , circular tubes C2 could continue in resisting the applied load to 460.8 kN. The numerical values of the peak load were 429.0 kN and 774.0 kN for square tubes types S1 and S2 respectively while the estimation values for circular tubes C1 and C2 were 459.0 kN and 476.0 kN respectively (Table 5). The maximum difference between the experimental and numerical values is around 9% (Fig.4 a).

Table 5 Experimental and numerical values of columns' load capacity (kN)

Specimen No.	S1	S2	C1	C2
1	464.0	751.0	410.9	506.0
2	470.0	740.0	537.5	415.6
Average	467.0	745.5	474.2	460.8
FEM	429.0	774.0	459.0	476.0

The failure modes of the experimental columns of square tubes S1 and S2 are local buckling and corner splitting at mid-height of the column followed by buckling respectively,while crushing at column's end is the failure mode of the circular columns. The failure modes using finite element simulattions are shown in Fig.4b. The failure modes by analyses also reflect good agreement with failure modes observed experimentally for square and circular columns. It is noted that the splitting around the corner of tubes in S2 observed experimetnally does not appear in FEM analyses as the program has not designed to display the progress of damage or crack in the FRP composite. The high stress zone which is appeared at the end of the circualr tubes shows the initiation of the failure in the circualr tubes.

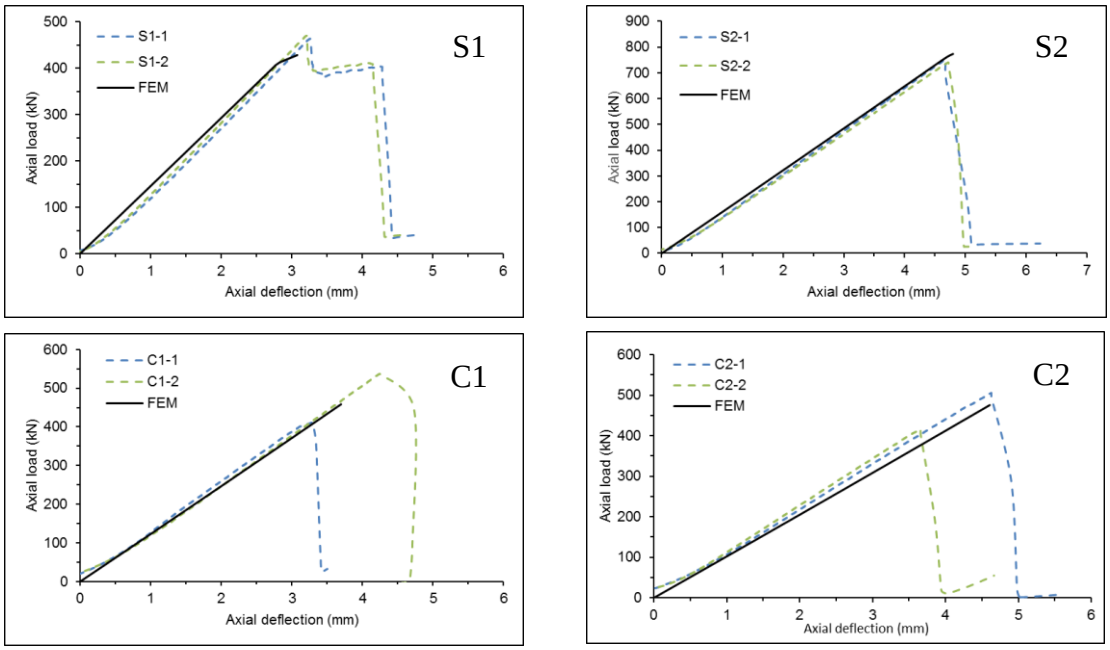

Figure 3 Finite element simulation

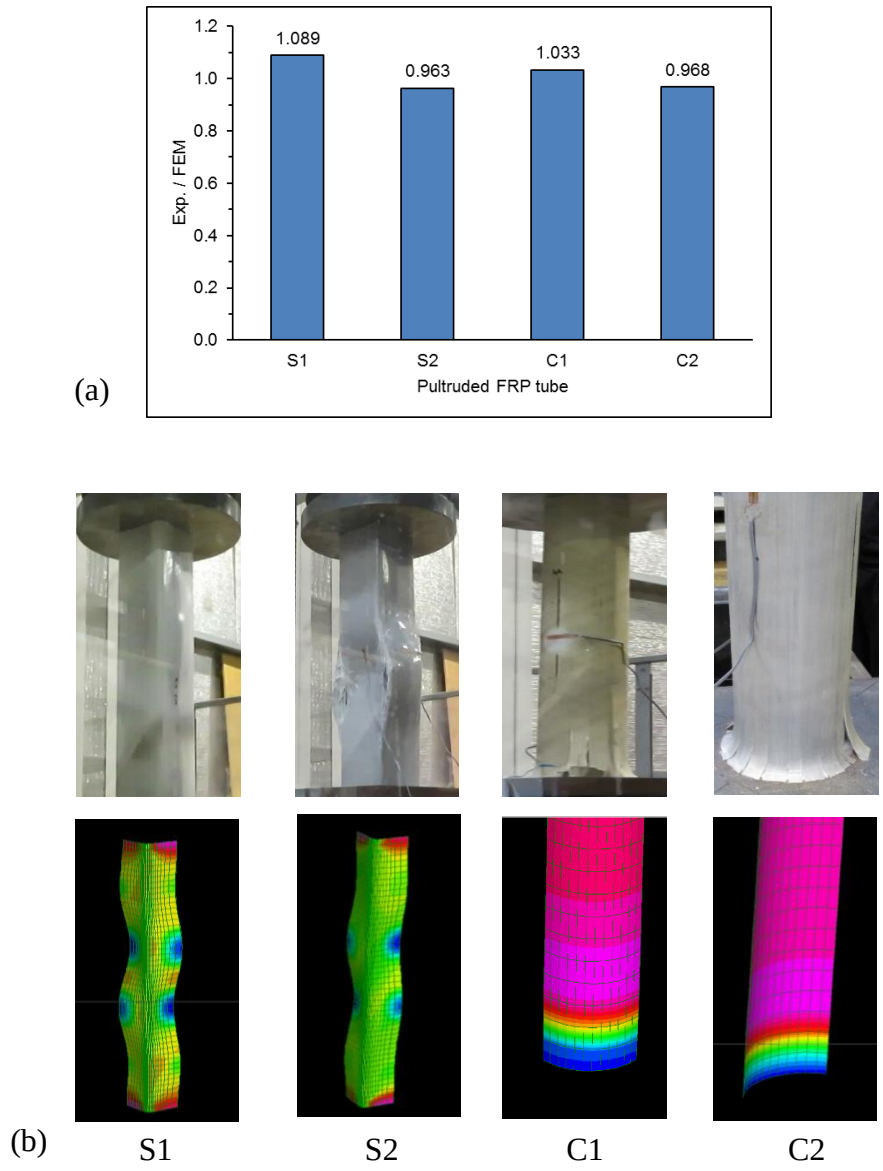

Figure 4 (a) Load capacity of pultruded FRP tubes and (b) Experimental and analytical failure modes.

5. Conclusions

This study has shown properties of four types of square and circular pultruded FRP tubes in shapes of the in finite element simulation. Also, finite element modeling of FRP columns is presented. Then, the performances of finite element models have been reported. Based on the results obtained from the experimental work and finite element simulation, the following findings can be drawn:

- The instability condition due to buckling controls the load carrying capacity of the square pultruded FRP tubes while the axial behaviour of the circular pultruded FRP tubes is influenced by the fibre orientation.
- The performance of finite element simulation using the laminate method provides acceptable results compared with experimental results.
- The peak load expectation using the first ply failure through the Tsai-Wu criterion coincided well with the results of the experimental columns (maximum difference of 9

%). The failure modes presented through FEM are in good agreement with those noted experimentally.

References

Abdelkarim, OI & Elgawady, MA 2015, 'Analytical and Finite-Element Modeling of FRP-Concrete-Steel Double-Skin Tubular Columns', *Journal of Bridge Engineering*, vol. 20, no. 8.

Barbero, E & Tomblin, J 1994, 'A phenomenological design equation for FRP columns with interaction between local and global buckling', *Thin-Walled Structures*, vol. 18, no. 2, pp. 117-31.

Barbero, EJ 2017, *Introduction to composite materials design*, Third edn, CRC Press, Boca Raton, Fla.

Carrion, JE, Hjelmstad, KD & LaFave, JM 2005, 'Finite element study of composite cuff connections for pultruded box sections', *Composite Structures*, vol. 70, no. 2, pp. 153-69.

Daniel, IMI, O. 2006, *Engineering mechanics of composite materials*, 2nd edn, Oxford University Press, New York.

Guades, E, Aravinthan, T & Islam, MM 2014, 'Characterisation of the mechanical properties of pultruded fibre-reinforced polymer tube', *Materials & Design*, vol. 63, pp. 305-15.

Hany, NF, Hantouche, EG & Harajli, MH 2016, 'Finite element modeling of FRP-confined concrete using modified concrete damaged plasticity', *Engineering Structures*, vol. 125, pp. 1-14.

Hassan, NK & Mosallam, AS 2004, 'Buckling and ultimate failure of thin-walled pultruded composite columns', *Polymers and Polymer Composites*, vol. 12, no. 6, pp. 469-81.

Jiang, J-F & Wu, Y-F 2012, 'Identification of material parameters for Drucker–Prager plasticity model for FRP confined circular concrete columns', *International Journal of Solids and Structures*, vol. 49, no. 3, pp. 445-56.

Kollár, LP 2002, 'Buckling of unidirectionally loaded composite plates with one free and one rotationally restrained unloaded edge', *Journal of Structural Engineering*, vol. 128, no. 9, pp. 1202-11.

Kollár, LP 2003, 'Local buckling of fiber reinforced plastic composite structural members with open and closed cross sections', *Journal of Structural Engineering*, vol. 129, no. 11, pp. 1503-13.

Kollár, LP & Springer, GS 2003, *Mechanics of Composite Structures*, Cambridge University Press, New York, UNITED STATES.

Module7:Strength and Failure Theories 2014, http://nptel.ac.in/courses/105108124/pdf/Lecture_Notes/LNm7.pdf>.

Puente, I, Insausti, A & Azkune, M 2006, 'Buckling of GFRP columns: An empirical approach to design', *Journal of Composites for Construction*, vol. 10, no. 6, pp. 529-37.

Ragheb, WF 2017, 'Development of closed-form equations for estimating the elastic local buckling capacity of pultruded FRP structural shapes', *Journal of Composites for Construction*, vol. 21, no. 4, p. 04017015.

Teng, J, Xiao, Q, Yu, T & Lam, L 2015, 'Three-dimensional finite element analysis of reinforced concrete columns with FRP and/or steel confinement', *Engineering Structures*, vol. 97, pp. 15-28.

Youssf, O, ElGawady, MA, Mills, JE & Ma, X 2014, 'Finite element modelling and dilation of FRP-confined concrete columns', *Engineering Structures*, vol. 79, pp. 70-85.

Zureick, A & Scott, D 1997, 'Short-term behavior and design of fiber-reinforced polymeric slender members under axial compression', *Journal of Composites for Construction*, vol. 1, no. 4, pp. 140-9.